

A displacement spindle in a micro/nano level

Kuang-Chao Fan^{1,2}, Zi-Fa Lai¹, Peitsung Wu¹,
Yung-Chang Chen¹, Yejin Chen² and Gerd Jäger³

¹ Department of Mechanical Engineering, National Taiwan University, Taipei, Taiwan

² School of Instrument Science and Opto-Electronic Engineering, Hefei University of Technology, Anhui, People's Republic of China

³ Institute of Process Measurement and Sensor Technology, Technische Universität Ilmenau, Ilmenau, Germany

E-mail: fan@ntu.edu.tw

Received 26 September 2006, in final form 4 December 2006

Published 8 May 2007

Online at stacks.iop.org/MST/18/1710

Abstract

This paper presents two micro/nano level displacement sensors, which consist of a mini LDGI (linear diffraction grating interferometer) and a focus probe. These two sensors are integrated into the spindle system of a micro/nano-CMM. This micro/nano spindle system is fixed on a rectangular granite bridge to achieve the z -axis function. The motion of the spindle is driven by an ultrasonic motor on a precision cross-roller slide. Its displacement is fed back by the LDGI. A DVD pick-up head is modified with its S-curve principle as the non-contact focus probe. Mounting the probe onto the spindle head, it is possible to achieve a large displacement and nanoresolution measuring spindle system with a feedback nanomotion control scheme. After accuracy calibration and error compensation, the spindle motion to 10 mm can perform 10 nm positioning accuracy and 30 nm measurement accuracy. Experiments on some ultraprecision profiles have shown the capability of this spindle system.

Keywords: linear diffraction grating interferometer, focus probe, ultrasonic motor, CMM

(Some figures in this article are in colour only in the electronic version)

1. Introduction

The term 'precision nanometrology' was proposed by Gao [1], who considered it as the science of dimensional measurement and motion measurement with 100 nm to 0.1 nm resolution/uncertainty within a range of micrometres to metres. In the engineering field, the degree of precision is often related to the ratio (in this paper, it is called the precision ratio) of resolution/uncertainty to range. In the extreme case, the precision ratio of 0.1 nm m⁻¹ (10⁻¹⁰) could be too strict to reach. However, if the resolution/uncertainty could be considered to be 10 nm and the range centimetres, the corresponding precision ratio of 10⁻⁶ (10 nm cm⁻¹) would be possible. In more general terms, this precision ratio can be expressed by tolerance to scale. In fact, most of the current technologies in manufacturing miniature parts are within this

category, such as the MEMS, energy beams or microEDM. Parts that can be produced can be such as micro grooves, micro nozzles, micro lens, etc. In addition, the need of accuracy in precision engineering is more important than that of resolution. In this paper, it is called 'micro/nano-technology', or more specifically 'micro precision technology', for the science and technology dealing with 100 nm to 10 nm accuracy/uncertainty and 1 nm resolution within a range of micrometres to centimetres. This is regarded as an immediate range that engineering technology can gradually enter into from a top-down approach.

In the development of micro/nano profile measurement, the precision measurement probe and displacement sensor are the most important modules [2]. For most long stroke and nanomotion stages, the high cost laser interferometer is commonly used as the displacement feedback sensor instead

of the general grating scale [12, 13]. However, the grating scale has two distinct advantages in accuracy over the laser interferometer: (1) immunity to atmospheric variations and (2) does not use a reflecting mirror and is therefore immune to the manufacturing tolerances and costs of machined mirrors [14]. Ishii and Nishimura developed a diffraction grating interferometer on a rotary encoder to achieve nanometre resolution. This system was then modified with dual heads to compensate for the tilting error in Cannon's laser encoder [3, 4]. Wu *et al* developed a double diffraction linear encoder to permit higher tolerance in angular errors during the motion [5]. This system is, however, never applied to the motion control. In this research, a mini linear diffraction grating interferometer (LDGI) system has been developed with the concept of common-path and high head-to-scale tolerance with respect to a fine pitch holographic grating scale to accomplish nanometre resolution. The focus and autofocus optical probes modified from a commercial DVD pick-up head have been carried out by Fan *et al* [6, 7] for quite a long time. A mechanical design for the case of the focus probe is implemented in the current research to make its appearance more like a real probe. Nanomotion control is often focused on the piezoelectric transducer (PZT) stage with a limited stroke [8]. Many long stroke with fine motion stages are built up by two stages, i.e. a long motion stage with a servomotor and a micro motion stage with PZT. A single stage possessing both long stroke and fine motion for the spindle motion of a micro-CMM has been introduced by Fan *et al* [9]. In this paper, a modified design using a higher tolerance LDGI, new spindle structure and new motion control scheme is proposed. Accurate positioning can be achieved by three velocity steps corresponding to large stroke, small stroke and fine stroke motions, respectively [10]. Experimental results show the feasibility of both sensors and the integrated spindle system.

2. Principle of long stroke and nanopositioner

A long stroke to a nanometre positioning stage will consist of three parts: a nanoresolution displacement sensor (LDGI), a nanomotion ultrasonic motor (HR4) and a precision cross-roller slide.

2.1. The ultrasonic linear stage

Most positioning technologies have to compromise between the stroke length and the positioning precision (accuracy + uncertainty). For the long-stroke motion, usually driven by the servomotor and detected by a linear scale, the positioning precision is limited to only the micrometre order. For the fine motion, usually driven by the PZT actuator and detected by the capacitance sensor, the stroke is limited to only several hundreds of micrometres. This study aims for a long stroke while possessing fine motion achieved by a single stage. Figure 1 shows the configuration of the proposed stage. The moving slide is supported by two cross-roller guides. This precision cross-roller slide is made by THK Co. of Japan. The actuator system consists of an ultrasonic motor (model HR-4) and a drive amplifier (model AB2), made by Nanomotion Co. of Israel. These two components are combined to create the piezoelectric effect. This effect converts an electrical field

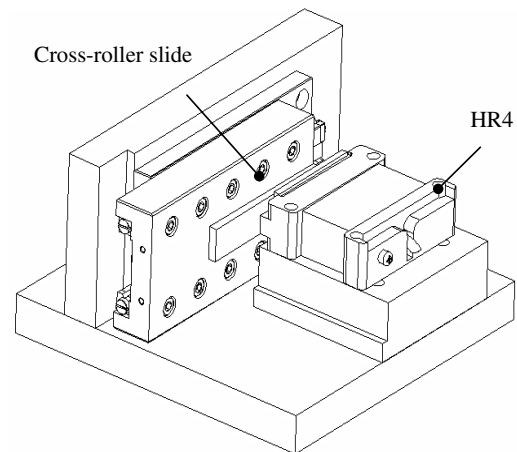


Figure 1. Structure of the long stroke and fine motion stage.

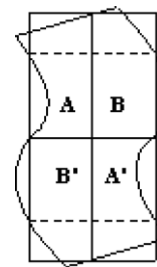


Figure 2. Motion mode of PCLM.

to a mechanical motion. The important role of operation is played by the four piezo elements of the HR-4 motor. When the voltage is applied across the element in a precise sequence, the edge of the piezo element generates an elliptical motion, which is the vector sum of the bending mode and the longitudinal mode, as shown in figure 2. This elliptical motion then drives the stage by a friction force to create a linear motion. The AB2 driver possesses three modes. The ac mode creates continuous steps for long travel with moderate speed to the approaching point, around $100\ \mu\text{m}$ before the target position. The gate mode follows with a pulse command in time interval at low speed to drive the stage to around $200\ \text{nm}$ distance before the target point. Finally, the dc mode can be activated with variable voltages enabling the moving stage to access within $5\ \text{nm}$ of the target point.

2.2. Principle of the high tolerance linear diffraction grating interferometer

The position feedback of the spindle motion in the z -axis is detected by the principle of a linear diffraction grating interferometer with $1\ \text{nm}$ resolution, as shown in figure 3. The laser diode emits a linearly P-polarized laser beam with $635\ \text{nm}$ wavelength. With the emitted angles equal to the grating's ± 1 diffraction angles, the input beams will be reflected back through the same path to mirrors 1 and 2. Passing through respective PBS (1 or 2), each beam will change to a P-beam again. Through a series polarization phenomenon the left arm beam will arrive at PD1 with a P-polarized beam and at PD2 with a S-polarized beam, and at PD3 with 45° and at PD4 with

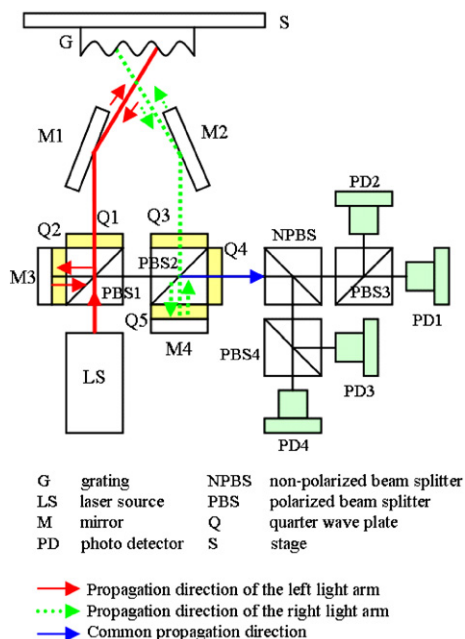


Figure 3. Optical system of LDGI.

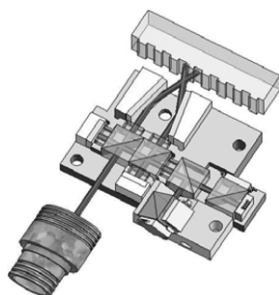


Figure 4. 3D assembly of LDGI.

135° polarized beams, respectively. The right arm beam will also eventually arrive at PD1, PD2, PD3 and PD4 with the same polarization as the left arm beam. The intensity of each photodetector can be expressed by

$$I_{PD1} = A [1 - \sin(2\Delta\omega \cdot t)] \tag{1}$$

$$I_{PD2} = A [1 + \sin(2\Delta\omega \cdot t)] \tag{2}$$

$$I_{PD3} = A [1 + \cos(2\Delta\omega \cdot t)] \tag{3}$$

$$I_{PD4} = A [1 - \cos(2\Delta\omega \cdot t)]. \tag{4}$$

Accordingly, by the detection of the phase variations of a beat frequency signal, we can measure the displacement of grating movement. Based on the Doppler effect, when the grating moves $d/2$, the beat frequency signal has a phase variation of periodicity (2π). With the holography grating of $1200 \text{ line mm}^{-1}$, there is a pair of orthogonal signals every 416 nm according to equations (1)–(4). With a simple waveform subdivision technique, we can easily reach 1 nm resolution. All the optics are selected as small as possible from the Edmund Scientific Co. Figure 4 plots the 3D assembly of this mini LDGI and figure 5 shows its photo with a physical dimensions of about $50 \times 30 \times 30 \text{ mm}^3$.

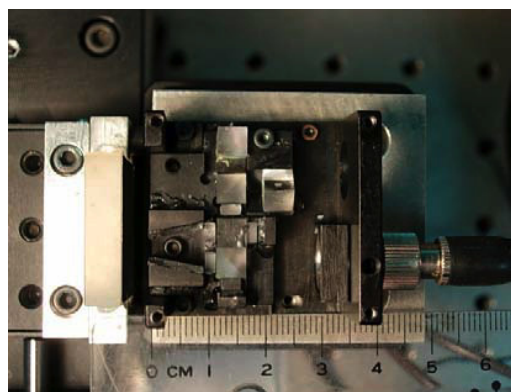


Figure 5. Photo of the LDGI.

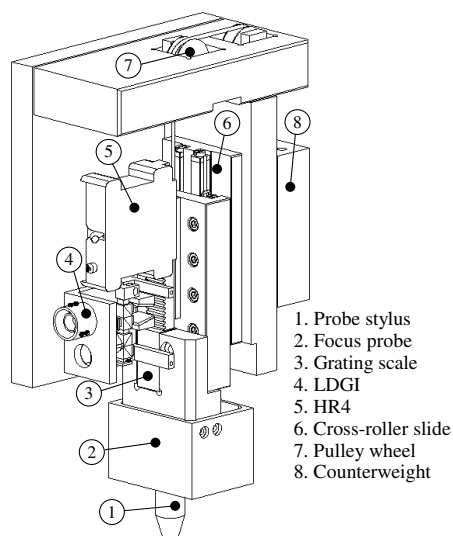


Figure 6. Structure of the Z-probe system.

Improving on the previous system in which the input laser beam is normal to the gratings [6], this paper presents a new LDGI where the laser beams are projected to the gratings from the ± 1 diffraction angles. The diffracted beams can thus return on the same light paths. In this design, the reflected beam of each path has a common axis with its emitted path. This common path principle allows higher tolerances to the yaw, roll and two straightness errors during the linear motion of the grating scale than the previous design [9]. Therefore, high head-to-scale tolerance can be assured [11].

2.3. Design of the z-axis spindle system

In the spindle mechanism, the cross-roller slide of figure 1 with 10 mm travel is used as the main moving stage. The actuator axis, grating axis and probe axis are aligned along the same axis, which conforms to the Abbe principle. The construction of the z-axis spindle system is shown in figure 6. The counterweight design minimizes the motion of the mass centre. The mounting bases of the mini LDGI and HR4 are separate (not shown in the figure), which can remove the influence of measuring equipment affected by the induced vibration of an actuator.

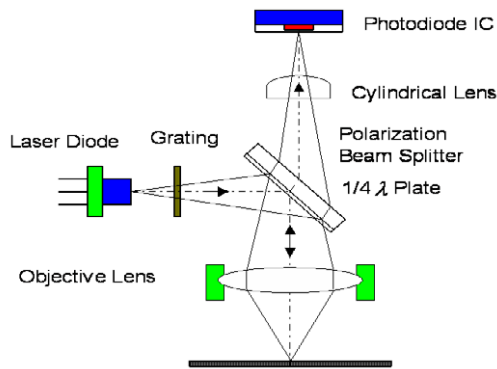


Figure 7. Optical system of the focus probe.

3. The focus probe

This research aims to develop a low cost optical probe with the measurement capability in the nanometre range. The pick-up head of a commercial DVD player was adopted based on its principle of focus error, as shown in figure 7. In this system, the focusing signal is detected by the astigmatism method. At the focal plane, the spot is a pure circle. When the object moves up or down away from the focal plane, the spot appears elliptical with different orientations. The corresponding FES provides an S-curve signal proportional to the object movement. A previous study has shown that the accuracy of the full linear range of the S-curve can reach 30 nm. However, if the linear range is selected in the vicinity of the linear centre point, the linearity error can be reduced to within 10 nm. For detailed principle, calibration and applications, one can refer to the authors' paper [6]. In this work, we just modify the pick-up head by adding an extended stylus to make it more of a probe shape, as shown by components 1 and 2 in figure 6.

4. Integrated control system

4.1. Motion control

Motion control of the spindle is actuated by the HR4 ultrasonic motor and feedback by the LDGI signal in three control modes: ac, gate and dc. In the ac mode, a constant voltage of 39.6 kHz frequency is applied to the stage. The velocity is related to the applied voltage. Figure 8 shows its characteristic curve. It can be seen that high speed occurs when the voltage is above 2.5 V. In this micro/nano accuracy spindle, a low voltage is recommended in order to sample the high rate signals of the LDGI accurately. After experiments, a low velocity response of $0.25 \text{ V}/(\text{mm s}^{-1})$ was selected as the motion control parameter for the ac mode.

In the gate mode, a low voltage was given to the AB2 driver in a short interval so that the stage could move with each step less than 300 nm. Experiments show that with an applied voltage of 0.8 V, the average step can achieve around 217 nm. Lastly, in the dc mode, the displacement is proportional to the supplied voltage. Experiments show that when the voltage changes from 0 to 10 V, the stage can move 300 nm if the friction is small. Because the friction will not be stable over the full range of 10 mm motion, the feedback

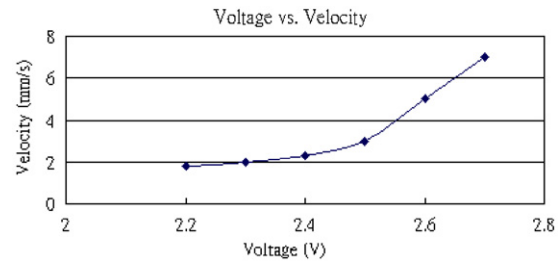


Figure 8. Velocity to voltage relationship in ac mode.

control is important to command the stage to the required position.

The whole positioning control is actuated in three steps. The ac mode drives the stage to the position before the target of about $40 \mu\text{m}$, the gate mode then follows up to move the stage to the position before the target of about 100 nm and the dc mode will lastly carry out the final positioning to the target with error less than $\pm 5 \text{ nm}$.

4.2. Signal process of the LDGI

Two main electronic circuits are designed for the signal process of the four-channel LDGI output, as given by equations (1)–(4). These are the orthogonal signal adjustment circuit and the up/down counter circuit. The schematic diagram of a signal process circuit is shown in figure 9.

In the orthogonal signal adjustment, the front end includes an $I-V$ converter and a differential amplifier. The back end circuit provides the auto-orthogonal function to tune the two waveforms to precisely 90° phase shift. The up/down counter is adopted from a NI 6016 DAQ counter IC, which has a Schmitt trigger IC and a HCTL-2032 IC (made by Agilent Co.). The latter is a 32-bit register with bandwidth 6 MHz. Each count is equivalent to one quarter of the wavelength of the LDGI output. The holography grating has a pitch of 833 nm. The orthogonal signals reduce the wavelength to 416 nm. Each count is, therefore, equivalent to 104 nm of the grating scale movement. The residual incomplete cycle will be detected by an A/D converter for the subdivision process. A precision 10-bit A/D converter can easily divide the signal to 0.4 nm resolution.

4.3. Signal tests

The performance of the orthogonal signal adjustment circuit was tested by the Lissajous plot. As seen in figure 9, orthogonal signals are always detected by the A/D converter. For the forward motion the phase shift is 90° , while for the reverse motion the phase shift will be -90° . Figure 10 shows that the Lissajous circle can always be compensated for both motions.

4.4. System integration

The integrated control system of the spindle includes a LDGI displacement sensor, a sinusoidal waveform signal counting circuit HCTL-2032, an ultrasonic HR4 motor with the AB2 drive and a DVD probe's FES circuit. Figure 11 shows the block diagram of the system structure. The DAQ (data

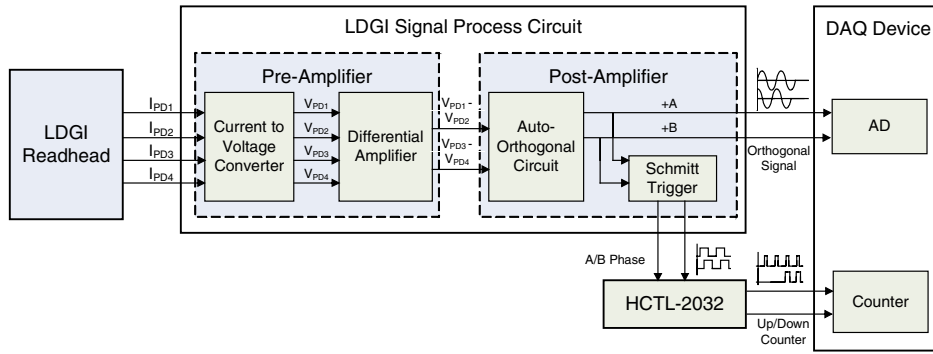


Figure 9. LDGI signal process diagram.

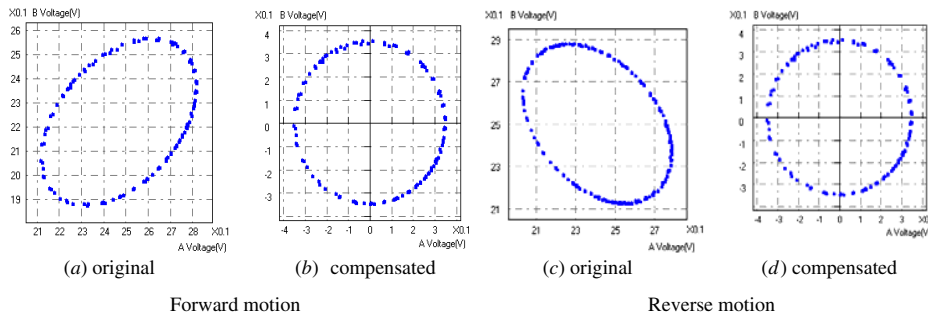


Figure 10. Orthogonal signal compensation tests.

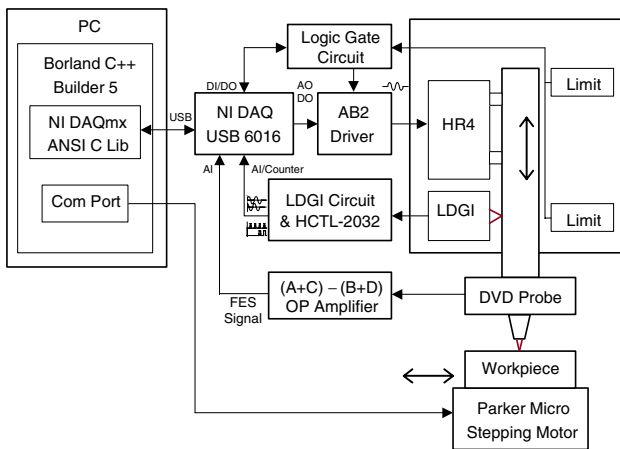


Figure 11. The block diagram of the control system.

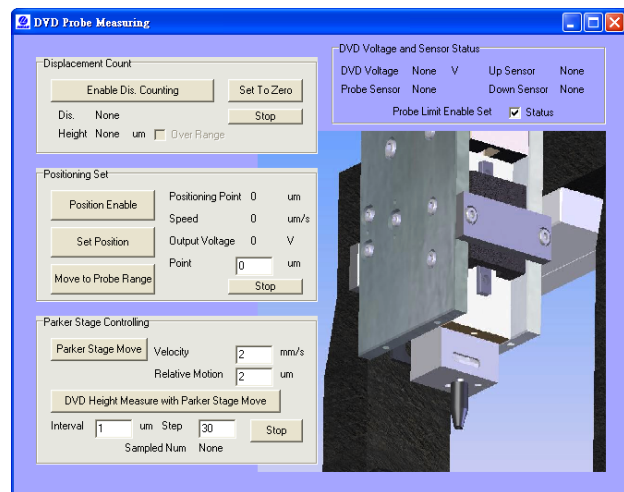


Figure 12. Screen of measurement system.

acquisition) card made by National Instrument Co. (model NI USB 6016) is to interface signals to a PC. The software program is developed with Borland C++ Builder. The spindle moves up and down according to the surface profile of the workpiece. The focus probe outputs the FES to drive the HR4 motion until the focal point is reached. The LDGI then takes the position reading. A micro stepping motor driven stage, made by Parker Co., provides the x -motion of the workpiece so that its surface profile can be scanned automatically.

In this system integration, the DVD focus probe plays the most important role for precision positioning of the spindle and precision measurement of the workpiece profiles. As the spot size of the focused laser beam is only $0.8 \mu\text{m}$, it can easily detect the profile variation of a very fine groove width.

Because the spindle can be moved in very fine steps of around 5 nm in the dc mode of the HR-4 motor, the linear range of the focus probe S-curve can be set to only $\pm 1 \mu\text{m}$ so that the linearity error of the probe can be controlled to less than 10 nm , as indicated in section 3. This FES signal is fed back to the motor to determine the stop command. In practice, the stopping point will not be exactly at the zero FES position. A linear interpolation will assist to compensate the out-of-focus error. The LabVIEW program can help us design a user-friendly pictorial/text screen on the monitor, as shown in figure 12. Although the focusing principle is independent of the material of the measured piece [7], the final position will

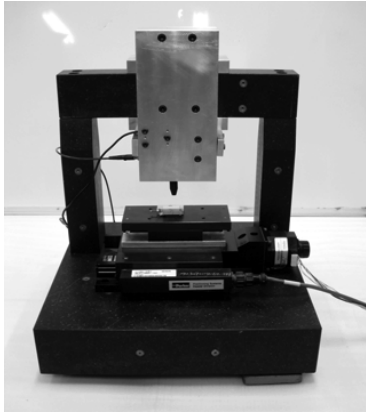


Figure 13. Experimental setup.

never arrive at the focus point. The S-curve calibration with respect to different materials is still necessary [6].

5. Measurement results

The whole spindle system is mounted onto the granite bridge of a micro/nano-CMM, as shown in figure 13. The experiment first aims at the positioning test of the z -axis, and then goes on to measure the micro/nano parts.

5.1. Positioning test of the Z -spindle system

A SIOS MI-5000 laser interferometer was used to calibrate the positioning accuracy of the z -axis movement. The distance of travel is 10 mm with every 1 mm step. Figure 14 shows the accuracy plots before and after the error compensation. Initial results show a linear trend to a maximum positioning error of $3.36 \mu\text{m}$. The reason for inaccuracy is the alignment error of the SIOS laser interferometer with respect to the z -axis motion. This can be easily compensated by removing the slope in the software, and the compensated error can be within $\pm 10 \text{ nm}$.

The characteristics of the stage composed of the HR-4 motor, AB2 drive, linear slide (NSK Co.) and LDGI feedback sensor have been studied in previous work [9]. It indicated that the repeatability could be influenced by four factors, namely, the straightness of the guideway, the quality of the hologram grating (Edmundoptics Co.), the quality of the optics used in the LDGI and the stability of the ambient temperature and the ground vibration. In this Z -spindle system, the HR-4, AB2, slide, grating and optics are all adopted from the same companies as before. The environmental conditions are also

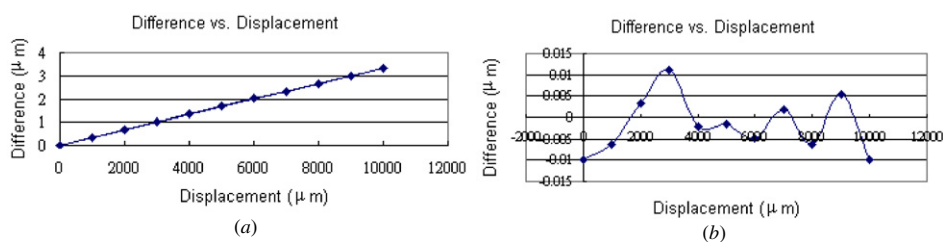


Figure 14. Z -axis positioning tests. (a) Initial results, (b) after compensation.

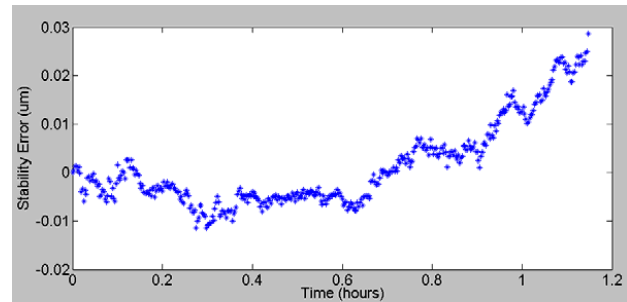


Figure 15. Long-term stability test of the focus sensor.

similar to the field of the previous test. Only the LDGI is a new design allowing better head-to-scale tolerance (please refer to section 2.2). The repeatability of the positioning accuracy of this Z -spindle system is slightly better than the previous work on the XY stage. On average, less than $\pm 20 \text{ nm}$ of 95% confidence level for the full travel of 10 mm could be controlled. With regards to the drift and long-term stability, at any fixed position the variation of LDGI readings (about 2 nm) is much smaller than that of the laser interferometer (about 10 nm). The drift error can be neglected. It has to be emphasized that this drift is largely dependent on the quality of the circuit board.

5.2. Tests of the focus sensor

Two tests have been conducted to prove the capability of the focus sensor. The first one is the long-term stability of the readings. Figure 15 shows that the variation of the focus sensor is within $\pm 10 \text{ nm}$ for a 1 h run. In practice, the actual time of each case measurement is less than 5 min. The drift error can be negligible. The second one is the accuracy test with a standard step height. This experiment was assisted by Professor Jäger at Technical University Ilmenau, Germany. The motion of a PTB step height (standard dimension of 69 nm) was driven by the NMM [12]. Figure 16 shows one of the measured results. Ignoring the edge effect on the optical probe, the calculated error is less than 1 nm . Repeatability tests for seven runs have also been conducted. The standard deviation is about 1.1 nm . This proves that the focus sensor is capable enough for micro/nano measurements.

5.3. Measurement examples

Some workpieces are adopted for measurements, namely, a $20 \mu\text{m}$ pitch linear scale, a CD and a holographic grating scale with a 833 nm pitch. The S-curve characteristics of

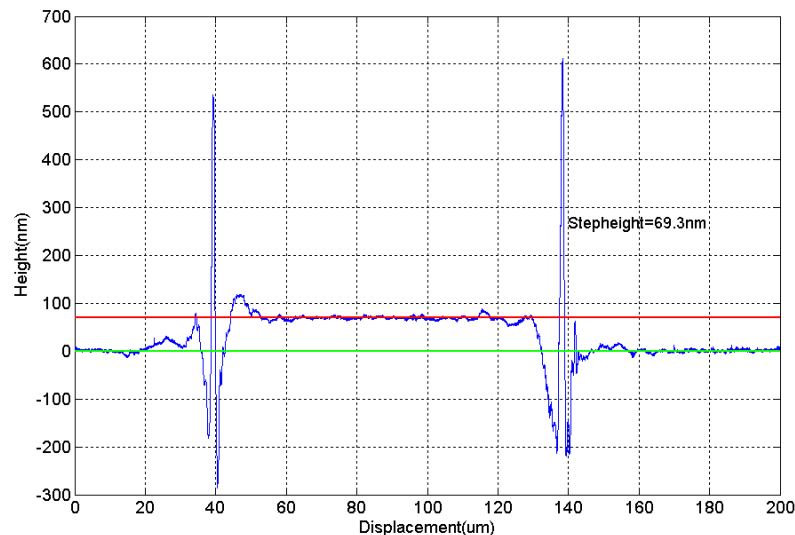


Figure 16. Step-height measurement of the focus probe.

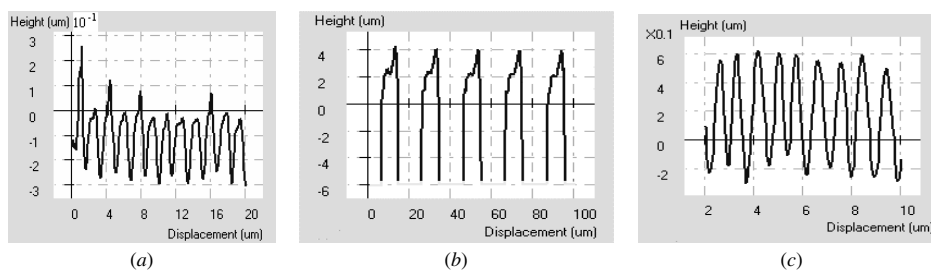


Figure 17. Measurement results. (a) CD profile, (b) linear scale and (c) holography grating.

the focus probe with respect to these four materials are tested beforehand. The micro stepping motor moves the workpiece every 50 nm step size. If the profile changes within the full S-curve range, the focus probe takes the readings directly. Figure 17 shows the measured surface profiles of the CD, linear scale and holographic gratings, respectively. The measured track spacing of the CD is about $1.6 \mu\text{m}$, and its peak-to-valley distance is about $0.19 \mu\text{m}$. From the specifications given by the manufacturer, the track distance of the investigated CD is $1.5 \mu\text{m}$ and the height is $0.2 \mu\text{m}$. There is an apparent period of $20 \mu\text{m}$ on the linear glass scale. Due to the substrate's transparent material, the height of the scale cannot be clearly measured. Its periodic cycle is, however, quite repeatable. The measured pitch of the holographic grating is about 842 nm , which is quite close to the nominal value of 833 nm .

6. Conclusions

Comparing to the servo (or linear) motor with the linear scale feedback system of general linear stages that allow a long stroke but limit to micrometre accuracy, this report presents a long stroke and an ultrahigh accuracy stage design with an ultrasonic motor and a LDGI feedback sensor. Building up into a Z-spindle system, it provides 10 mm travel to 1 nm resolution. Integrating the developed focus probe into the spindle, it can be used as the z -axis of a microcoordinate

Table 1. Performance specifications of the developed spindle system.

Spindle only	
Stroke length	10 mm
Minimum incremental step	5 nm
LDGI resolution	1 nm
LDGI drift	2 nm
Positioning accuracy	$\pm 10 \text{ nm}$
Positioning repeatability	$\pm 20 \text{ nm}$
Focus sensor only	
Linearity range	$\pm 1 \mu\text{m}$
Accuracy	$\pm 1 \text{ nm}$
Repeatability	$\pm 2 \text{ nm}$
Drift (1 h)	$\pm 10 \text{ nm}$
Integrated spindle system	
Measurement accuracy	$\pm 30 \text{ nm}$

measuring machine, or an independent automatic non-contact height gauge. Combining with a linear stage, this spindle system can scan surface profiles in a micro- to nano-variation level.

The overall performance indices of the current Z-spindle are summarized in table 1. Possible error sources could be due to (1) the straightness of the guideway, (2) the quality of the holographic gratings, (3) the quality of the optics, (4) the stability of ambient conditions, (5) heat generated by the motor, the laser and friction and (6) electrical drift of the circuit

boards. The major advantages of this developed system are high accuracy, long stroke, nanoresolution and especially low cost.

Acknowledgments

The authors wish to express their gratitude to the National Science Council of Taiwan and the National Natural Science Foundation of China for the grants for parts of this research.

References

- [1] Gao W 2005 Precision nanometrology and its applications to precision nanosystems *Int. J. Precis. Eng. Manuf.* **6** 14–20
- [2] Mckeown P 1998 Nanotechnology—special article *Proc. Nano-metrology in Precision Engineering (Hong Kong, 24–25 November)* pp 5–55
- [3] Nishimura T, Kubota Y, Ishii S, Ishizuka K and Tsukiji S M 1991 Encoder incorporating a displaceable diffraction grating *US Patent No 5038032*
- [4] Ishizuka K and Nishimura T 1992 Encoder with high resolving power and accuracy *US Patent No 5416085*
- [5] Wu C C, Chen Y C, Lee C K, Hsieh C T, Wu W J and Lu S S 1999 Design verifications of a linear laser encoder with high head-to-scale tolerance *Proc. SPIE* **3779** 73–82
- [6] Fan K C, Lin C Y and Shyu L H 2000 The development of a low-cost focusing probe for profile measurement *Meas. Sci. Technol.* **11** N1–7
- [7] Fan K C, Chu C L and Mou J I 2001 Development of a low-cost autofocusing probe for profile measurement *Meas. Sci. Technol.* **12** 2137–46
- [8] Shyu K K and Chang C Y 2003 Antiwindup controller design for piezoelectric ceramic linear ultrasonic motor drive *Proc. Industrial Electronics Conf.* vol 1 pp 341–6
- [9] Fan K C, Fei Y T, Yu X F, Chen Y J, Wang W L, Chen F and Liu Y S 2006 Development of a low cost micro-CMM for 3D micro/nano measurements *Meas. Sci. Technol.* **17** 524–32
- [10] Shen S M 2005 Fabrication of compact laser diffraction encoder system with high alignment tolerance *Master Thesis* National Taiwan University
- [11] Fan K C, Cheng F and Chen Y J 2006 Nanopositioning control on a commercial linear stage by software error compensation *Nanotechnol. Precis. Eng.* (ISSN: 1672-6030) **4** 1–9
- [12] Hausottee T and Jäger G 2004 Traceable nanometrology with a nanopositioning and nanomeasuring machine *J. CSME* **25** 399–404
- [13] Peggs G N, Lewis A and Leach R K 2003 Measuring in three dimensions at the mesoscopic level *Proc. ASPE Winter Topical Meeting—Machines and Processes for Micro-scale and Meso-scale Fabrication, Metrology and Assembly (Florida, USA)* pp 53–7
- [14] Burton G L and Burton P J 1996 X-Y-Theta positioning mechanism *US Patent 5,523,942*